Available online at www.sciencedirect.com
SCIENCE DIRECT®
Earth and Planetary Science Letters 248 (2006) 15–29
EPSL
www.elsevier.com/locate/epsl

Underlying causes for long-term global ocean $\delta^{13}C$ fluctuations over the last 1.20 Myr

B.A.A. Hoogakker [a,*], E.J. Rohling [a], M.R. Palmer [b], T. Tyrrell [a], R.G. Rothwell [a]

[a] National Oceanography Centre, Southampton, University of Southampton, SO14 3ZH, UK
[b] School of Ocean and Earth Sciences, University of Southampton, SO14 3ZH, UK

Received 21 December 2005; received in revised form 21 April 2006; accepted 1 May 2006
Available online 11 July 2006
Editor: M.L. Delaney

Abstract

Pleistocene stable carbon isotope ($\delta^{13}C$) records from surface and deep dwelling foraminifera in all major ocean basins show two distinct long-term carbon isotope fluctuations since 1.00 Ma. The first started around 1.00 Ma and was characterised by a 0.35‰ decrease in $\delta^{13}C$ values until 0.90 Ma, followed by an increase of 0.60‰ lasting until 0.50 Ma. The subsequent fluctuation started with a 0.40‰ decrease between 0.50 and 0.25 Ma, followed by an increase of 0.30‰ between 0.25 and 0.10 Ma. Here, we evaluate existing evidence and various hypotheses for these global Pleistocene $\delta^{13}C$ fluctuations and present an interpretation, where the fluctuations most likely resulted from concomitant changes in the burial fluxes of organic and inorganic carbon due to ventilation changes and/or changes in the production and export ratio. Our model indicates that to satisfy the long-term 'stability' of the Pleistocene lysocline, the ratio between the amounts of change in the organic and inorganic carbon burial fluxes would have to be close to a 1:1 ratio, as deviations from this ratio would lead to sizable variations in the depth of the lysocline. It is then apparent that the mid-Pleistocene climate transition, which, apart from the glacial cycles, represents the most fundamental change in the Pleistocene climate, was likely not associated with a fundamental change in atmospheric pCO_2. While recognising that high frequency glacial/interglacial cycles are associated with relatively large (100 ppmv) changes in pCO_2, our model scenario (with burial changes close to a 1:1 ratio) produces a maximum long-term variability of only 20 ppmv over the fluctuation between 1.00 and 0.50 Ma.

Keywords: long-term carbon isotope fluctuations; ventilation; production- and export ratio; modelling; mid-Pleistocene climate transition; mid-Brunhes event; Ocean Drilling Program; Joides Resolution; Site 502; Site 659; Site 758; Site 849; Site 1143; Site 982; Site 847

1. Introduction

Systematic oceanic carbon isotope ($\delta^{13}C$) shifts are commonly used indicators of change in the global carbon cycle, with research focussing on such shifts at the Cretaceous/Paleogene boundary [1], in the Miocene [2,3], and at the Palaeocene–Eocene boundary [4]. The main interest of this study concerns sustained long-term $\delta^{13}C$ shifts at timescales that exceed glacial/interglacial variability over the last 1.20 Myr, coincident with the possibly earliest onset of the Mid-Pleistocene climate transition [5]. In essence, the fluctuations considered here are background fluctuations that underlie the

* Corresponding author. Present address: University of Cambridge, Department of Earth Sciences, Downing Street, Cambridge, CB2 3EQ, UK. Tel.: +44 1223 33452; fax: +44 1223 33450.
E-mail address: bhoo03@esc.cam.ac.uk (B.A.A. Hoogakker).

0012-821X/$ - see front matter © 2006 Elsevier B.V. All rights reserved.
doi:10.1016/j.epsl.2006.05.007

superimposed $\delta^{13}C$ variability associated with the 41 to 100-kyr glacial cycles.

Two global long-term $\delta^{13}C$ fluctuations can be identified during the last 1.20 Myr in records from both surface dwelling (planktonic) and bottom dwelling (benthic) foraminifera from all major ocean basins (Fig. 1, Supplementary information 1). Planktonic foraminiferal $\delta^{13}C$ records reflect conditions in a thin surface layer with a high potential variability on regional scales while benthic foraminiferal $\delta^{13}C$ records are more indicative of long-term stabilised properties in the oceanic deep-water reservoir that forms >75% of the global ocean volume. Therefore we focus on the benthic foraminiferal $\delta^{13}C$ records.

During the last 1.20 Myr, benthic foraminiferal $\delta^{13}C$ records show similar long-term trends (i.e. trends exceeding variations on times scales up to and including glacial/interglacial time scales) (Fig. 2). The two long-term fluctuations recognized have been termed the Mid-Pleistocene $\delta^{13}C$ Fluctuation (MPCF; 1.00–0.50 Ma) and the Late-Pleistocene $\delta^{13}C$ Fluctuation (LPCF; 0.50–0.10 Ma). $\delta^{13}C$ differences between the sites are related to water-mass ageing and mixing (Fig. 2). Today, the $\delta^{13}C$ value of freshly formed North Atlantic Deep Water is ~1‰, decreasing to ~0‰ en route to the North Pacific, through mixing with Southern Ocean Water and continued remineralization of organic matter [11]. Despite these relative offsets between records from different basins, they all show the same systematic Pleistocene long-term $\delta^{13}C$ variability, thus confirming the global nature of these fluctuations (Fig. 2).

Initial explanations of the ca. 0.35‰ drop in $\delta^{13}C$ values at the start of the MPCF maintained that a drop in the mean ocean $\delta^{13}C$ was due to a one-time net addition of ^{12}C-enriched carbon to the world ocean [12]. This could have been caused by: (1) an increase in continental weathering and runoff; (2) an addition of organic matter to the ocean/atmosphere carbon reservoir from continental shelves; or (3) a global increase in aridity and decrease in the size of the biosphere across the 41 to 100-kyr transition [12]. The first two options were discarded as such processes would also enhance ocean nutrient concentrations and thus increase vertical $\delta^{13}C$ gradients and the spatial $\delta^{13}C$ gradient between the Atlantic and Pacific Oceans [13], whereas records suggest that these gradients remained relatively constant [12]. Raymo et al. [12] rule out a shift in the dominance of C3/C4 terrestrial ecosystems, as this would require a relatively large shift. In addition, the size of the terrestrial biosphere would have to decrease by more than 60% in order to explain the drop in $\delta^{13}C$ values at the start of the MPCF, which seems unlikely [12].

The MPCF is approximately coincident with the mid-Pleistocene Climate Transition (MPT), which is marked by an increase in mean global ice volume and a shift from 41-kyr to 100-kyr ice-age cycles [12]. The timing of the initiation of the LPCF can be broadly linked to the mid-Brunhes event which has also been associated with an increase in global ice volume [14]. It has been suggested that the ice-sheet expansion at the mid-Brunhes event might have been a reaction to changes in the global carbon cycle in relation to low-latitude upper ocean changes [15].

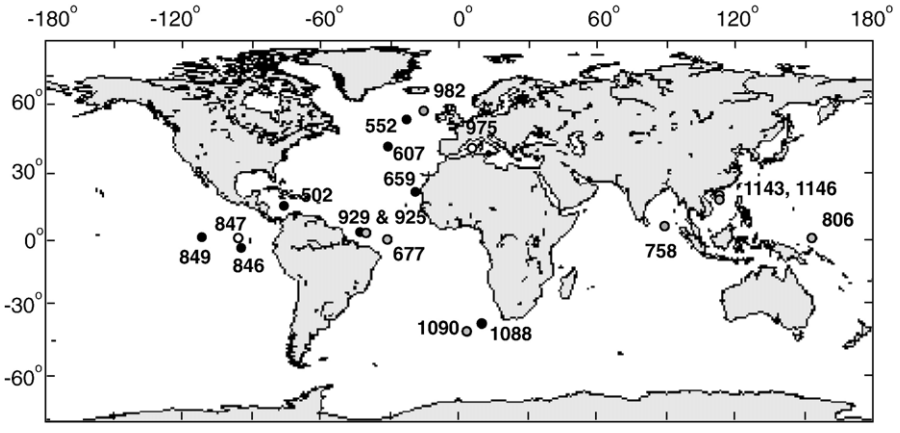

Fig. 1. Locations of all published records where, depending on the length of the record, either one or two of the long-term Pleistocene carbon isotope fluctuations can be recognized. Black circles represent locations with benthic foraminiferal $\delta^{13}C$ records; open circles sites with planktonic foraminiferal $\delta^{13}C$ records; and grey circles show locations with both benthic and planktonic foraminiferal $\delta^{13}C$ records. Foraminiferal $\delta^{13}C$ records are shown in Supplementary information 1.

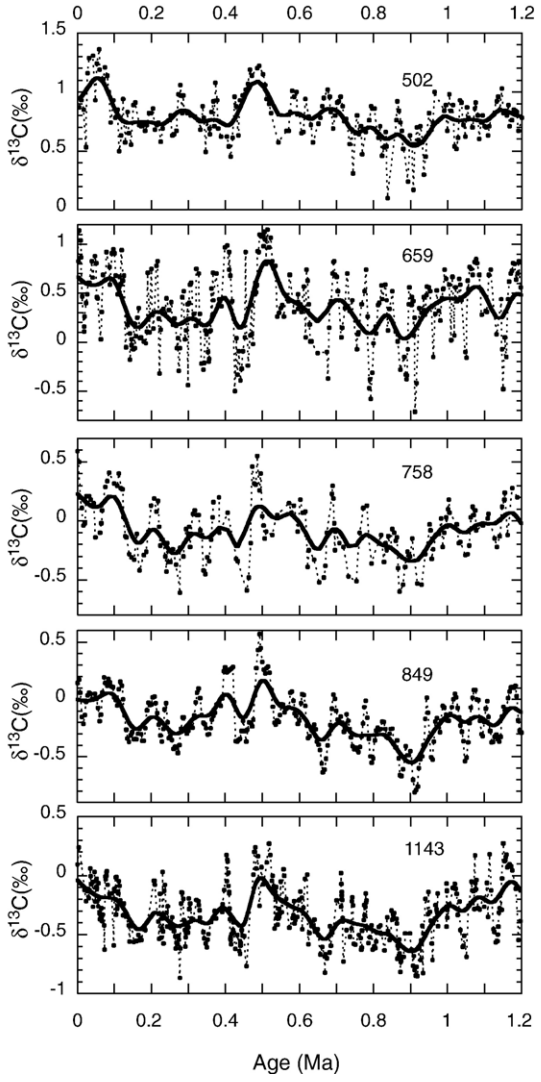

Fig. 2. Long-term stable benthic foraminiferal $\delta^{13}C$ records from the Atlantic Ocean (Site 659 [6]), Caribbean Sea (Site 502 [7]), the Indian Ocean (Site 758 [8]), the Pacific Ocean (Site 849 [9]), and, South China Sea (Site 1143 [10]). In order to illustrate $\delta^{13}C$ variations on larger than glacial/interglacial time-scales the individual records are smoothed with a 60 kyr moving Gaussian filter (thick black line, for details see Method).

Hence, alternative hypotheses in relation to the global carbon cycle need to be considered for the observed Pleistocene $\delta^{13}C$ shifts.

2. Method

2.1. Stacked benthic foraminiferal carbon isotope record

In order to assess the Pleistocene benthic foraminiferal $\delta^{13}C$ records, we compare several benthic foraminiferal $\delta^{13}C$ records (ODP Sites 502, 659, 758, 849, and 1143 [6–10]) that are all based on the same epibenthic foraminiferal species (*Cibicidoides wuellerstorfi*) (Fig. 2). Thus possible anomalies associated with infaunal habitats are avoided. The records were selected on the basis of the reliability of the respective age models and continuous coverage (average sample resolution <10 kyr and avoidance of records with repeated major (>30 kyr) age gaps) throughout the last 1.20 Myr. Other available benthic foraminiferal $\delta^{13}C$ records also show the long term $\delta^{13}C$ fluctuations, but were not used because they did not fulfil the above criteria. We also avoided using benthic foraminiferal $\delta^{13}C$ records from high productivity areas, as low carbonate ion concentrations may lead to $\delta^{13}C$ enrichment in foraminiferal calcite [16,17].

All records used for this study were standardized to a common timescale, with astronomically calibrated ages of 0.778 Ma (Matuyama/Brunhes) and 0.990 Ma (Upper Jaramillo) assigned to the magnetic reversal boundaries [18,19]. Ages for $\delta^{18}O$ stages are derived from [20] until $\delta^{18}O$ event 15.1 and then after [8,18, and,21] for older stages.

To elucidate the global trends, we constructed individual smoothed benthic foraminiferal $\delta^{13}C$ records, using a 60-kyr moving Gaussian filter to reduce variations on glacial/interglacial or shorter time scales (Fig. 2). A higher frequency filter picks up more of the glacial/interglacial variability, which we are explicitly excluding from this study. A lower frequency filter (100-kyr) interferes with the apparent timing (up to 20 kyr compared with the 60-kyr smoothing) of extremes that represent long-term changes in the $\delta^{13}C$ records. Hence the 60-kyr smoothing frequency is most suitable for examining long-term changes in the carbon cycle of the type considered here.

After smoothing, the filtered records were standardised to a modern value of 0.38‰ so that its present-day value matches the mean $\delta^{13}C$ value for total carbonate in recent deep-sea sediments [22] (Fig. 3). This shift is needed because our calculations require not only relative but also absolute values. The basis for shifting the filtered benthic foraminiferal $\delta^{13}C$ records is supported by the fact that the actual mean core-top value for the records used is nearly identical to the mean value for modern deep-sea sediments (~0.38‰) [22]. The very high level of agreement between the various standardised records again emphasises the systematic nature of the Pleistocene long-term $\delta^{13}C$ fluctuations, which affected both benthic and planktonic foraminiferal records in all major ocean basins (see Supplementary information 1). Finally, a mean value was calculated for the records in 1000 yr increments giving the standardised 'mean' record presented in Fig. 3.

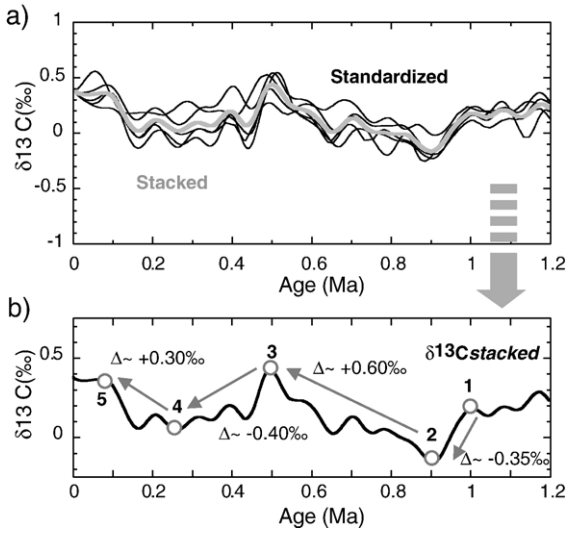

Fig. 3. (a) Smoothed benthic foraminiferal $\delta^{13}C$ records from Fig. 2 standardised to a modern value of 0.38‰ [22]. The thick grey line represents the standardised 'mean' or stacked benthic foraminiferal $\delta^{13}C$ record. (b) Quantification of the major changes in the stacked benthic foraminiferal $\delta^{13}C$ record between the five nodes.

Five 'nodes', marked in Fig. 3, identify major changes in the $\delta^{13}C$ values within the stacked benthic foraminiferal record. The first $\delta^{13}C$ fluctuation in $\delta^{13}C_{stacked}$, or the MPCF, started with a drop in $\delta^{13}C$ of ~0.35‰ between 1.00 and 0.90 Ma (nodes 1 and (2), followed by an increase of 0.60‰ between 0.90 and 0.50 Ma (nodes 2 and 3) (Fig. 3). The second fluctuation, or the LPCF, started with a drop in $\delta^{13}C$ of 0.40‰ between 0.50 and 0.25 Ma (nodes 3 and 4), followed by an increase of 0.30‰ from 0.25 to 0.10 Ma (nodes 4 and 5). Note, although the assignment of an age to node 4 is somewhat less obvious than for the other nodes, a precise date for this feature is not required in the models developed below.

2.2. Mechanistic box model

In order to evaluate possible causes for the two long-term $\delta^{13}C$ fluctuations we use the 3-box model of ocean nutrient and carbon cycling coupled to atmospheric carbon dioxide from Chuck et al. [23]. The 3-box model includes phytoplankton and the chemical tracers (state variables) of phosphate, dissolved inorganic carbon (DIC) and alkalinity. $CaCO_3$ dissolution is modelled without explicit sediment chemistry, but with a dynamic lysocline whose depth is calculated as a function of the carbonate ion concentration in the deep box. $CaCO_3$ burial is therefore calculated as a function of the $CaCO_3$ sinking flux and the fraction of the seafloor receptive to $CaCO_3$ burial (calculated from the lysocline depth and ocean hypsometry). The model also includes $DI^{12}C$ and $DI^{13}C$ as state variables in the ocean boxes, and $^{12}CO_2$ and $^{13}CO_2$ as state variables in the atmosphere to which it is coupled. Model runs were therefore executed with feedbacks between (1) ocean phosphate and organic export burial, (2) deep ocean carbonate ion concentration and $CaCO_3$ burial, and (3) $\delta^{13}C$ of seawater and $\delta^{13}C$ of the inorganic and organic carbon burial fluxes (F_{ino} and F_{org} respectively).

The model has open boundaries (river inputs and burial outputs) and is therefore not a closed system. Carbonate compensation is included in the model, with the model automatically converging towards a balance between river (weathering) inputs and $CaCO_3$ burial outputs over periods exceeding ~10 kyr (carbonate compensation *e*-folding response time). The model has no direct representation of the respiratory dissolution process because it contains no explicit sediments. It is however important to note that respiratory dissolution does not generally decouple the lysocline from the saturation horizon [24]. A detailed model description is presented in Supplementary information 2.

The following six scenarios are considered to explain the long-term $\delta^{13}C$ fluctuations:

1. $\delta^{13}C_{stacked}$ changes are driven by changes in the carbon isotopic ratio of the river input (δ_{riv}). These changes could be caused by changes in the relative weathering rates of organic and inorganic carbon or by a shift in the dominance of C3/C4 terrestrial ecosystems.
2. Changes in $\delta^{13}C_{stacked}$ reflect changes in the $\delta^{13}C$ of organic carbon buried (δ_{org}). δ_{org} variations can result from changes in fractionation during the formation of organic matter.
3. The changes in $\delta^{13}C_{stacked}$ are caused by changes in the isotopic composition of inorganic carbon buried (δ_{ino}). Possible causes for such changes could include changes in productivity in surface waters through changes in nutrient supply.
4. Changes in $\delta^{13}C_{stacked}$ reflect changes in the input of carbon through rivers (F_{riv}). Changes in F_{riv} could result from changes in the weathering rate of soils or rocks, or changes in the amount of weatherable carbon in the source rock or soil.
5. Fluctuations in $\delta^{13}C_{stacked}$ relate to variations in the organic and inorganic carbon burial fluxes (F_{org} and F_{ino}), either caused by (a) changes in burial preservation with the applied changes following the approximate global F_{org} and F_{ino} ratio of 1:4 [25], or (b) by changes in the production- and export rain ratio (ratio between organic and inorganic carbon

Table 1
Changes required in the 6 different scenarios in order to explain the MPCF and LPCF (see text for full details of different scenarios)

Scenario age (Ma)	~1.20–1.00	1.00–0.90 (nodes 1–2)	0.90–0.50 (nodes 2–3)	0.50–0.25 (nodes 3–4)	0.25–0.10 (nodes 4–5)
$\delta^{13}C$ of input and output (in ‰)					
Scenario 1 δ_{riv}	−3.9	−4.65	−3.60	−4.17	−3.55
Scenario 2 δ_{org}	−21.5	−15.0	−24.0	−19.5	−24.5
Scenario 3 mixing coefficient (relative to 1.20–1.00 Ma)	1.00	0.80	1.15	0.90	1.10
Input and output fluxes (g C yr^{-1}, $\times 10^{14}$)					
Scenario 4					
F_{riv} (4a)	2.40	3.05	2.39	3.00	2.60
F_{riv} (4b)	2.40	3.05	2.40	3.30	2.75
Scenario 5					
a) F_{org}, F_{ino} [δ1:4]	0.48 / 1.92	0.38 / 1.52	0.52 / 2.08	0.45 / 1.80	0.53 / 2.12
b) *P-ratio*	0.0299	0.0237	0.0324	0.0281	0.0314
Scenario 6					
a) F_{org}, F_{ino} [δ1:1]	0.48 / 1.92	0.39 / 1.83	0.50 / 1.94	0.46 / 1.90	0.51 / 1.95
b) *P-ratio*	0.0299	0.0285	0.0306	0.0296	0.0304

Scenario 3 shows the changes that are needed in vertical ocean mixing/productivity to reproduce the $\delta^{13}C_{stacked}$ fluctuations, relative to the ocean mixing values of 1.20–1.00 Ma (between 1.00 and 0.90 Ma vertical mixing was reduced to 80% compared to mixing between 1.20 and 1.00 Ma). Calculations for scenario 4 are split up in 4a (no nutrient changes) and 4b (nutrients allowed to change concurrently by 50%). Calculations for scenarios 5 and 6 are split up in 5a and 6a (driven by preservation changes with no carbonate compensation) and 5b and 6b (driven by changes in the production ratio [*P-ratio*] allowing carbonate compensation).

exported from the sea surface), with a ratio of change of 1:4.

6. $\delta^{13}C_{stacked}$ fluctuations are caused by variations in the organic and inorganic carbon burial fluxes (F_{org} and F_{ino}), again caused by (a) changes in burial preservation or (b) by changes in the production- and export rain ratio, but with a ratio of change of 1:1.

Changes in the carbon burial fluxes (scenarios 5 and 6) can be linked to changes in the rain rate (carbonate particles falling to the sea-floor) and preservation. Changes in the latter are likely a result of changes in dissolution linked to bottom water ventilation, and scenario 6a, with $\Delta F_{org}:\Delta F_{ino}=1:1$, in this context represents respiratory dissolution through an adherence to the stoichiometry of the schematic equations: $CH_2O+O_2 \Leftrightarrow CO_2+H_2O$ and $CaCO_3+CO_2+H_2O \Leftrightarrow Ca^{+}+2HCO_3^{-}$.

3. Results

The changes that are needed in the different parameters in order to establish the observed fluctuations in

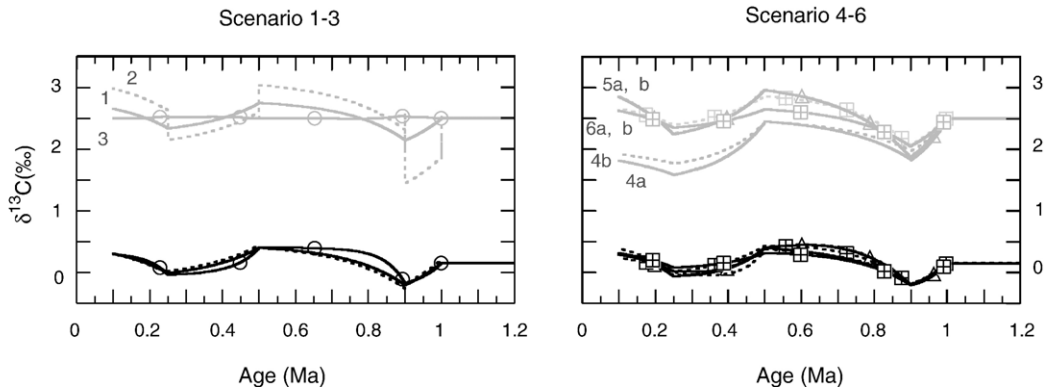

Fig. 4. Planktonic (grey) and benthic (black) foraminiferal $\delta^{13}C$ records for the six scenarios. Note that all benthic foraminiferal $\delta^{13}C$ records are narrowly constrained, whereas large differences can be observed between the different planktonic foraminiferal $\delta^{13}C$ records. For scenario 4 two calculations were executed where changes in the input of carbon through rivers is (a) not accompanied by simultaneous input of nutrients, and (b) supplemented by concurrent 50% changes in nutrient input. Numbers at the end of each $\delta^{13}C$-record indicate each scenario. For scenarios 5 and 6 two calculations were executed with burial changes caused by variations in (a) preservation and (b) the production ratio.

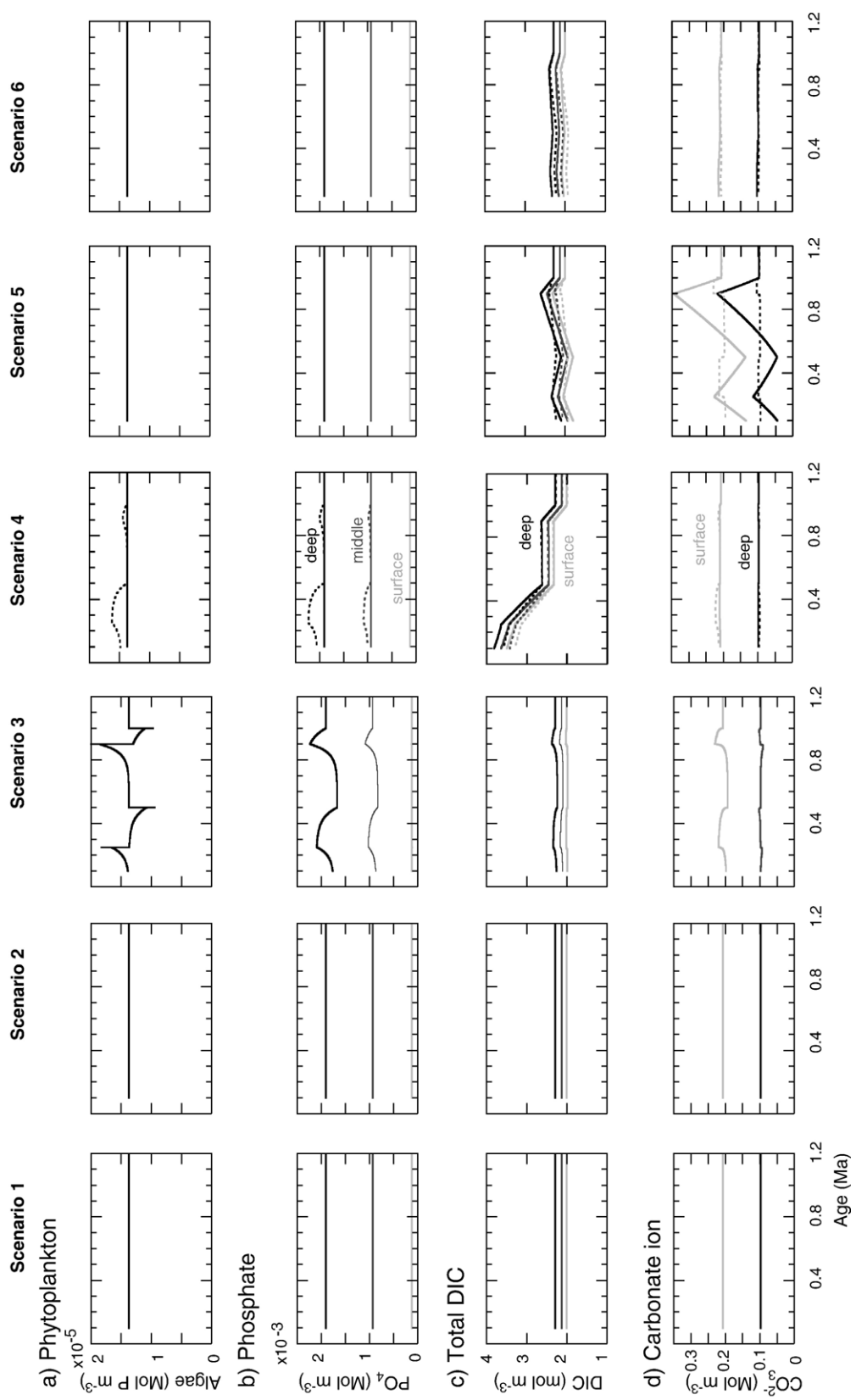
Scenario 1
Scenario 2
Scenario 3
Scenario 4
Scenario 5
Scenario 6
a) Phytoplankton
Algae (Mol P m-3)
x10-5
b) Phosphate
PO4 (Mol m-3)
x10-3
c) Total DIC
DIC (mol m-3)
d) Carbonate ion
CO32- (Mol m-3)
deep
middle
surface
Age (Ma)

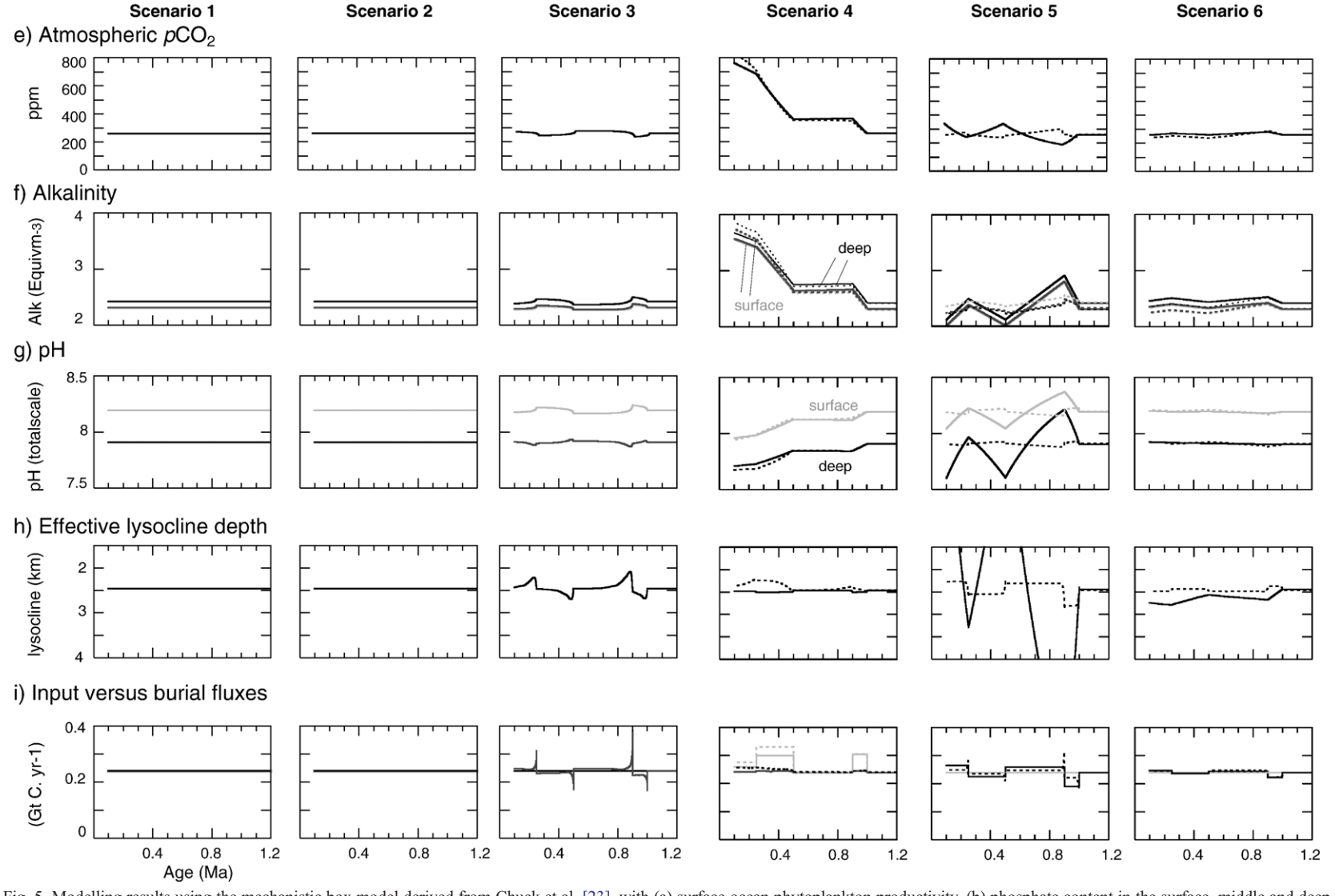

Fig. 5. Modelling results using the mechanistic box model derived from Chuck et al. [23], with (a) surface ocean phytoplankton productivity, (b) phosphate content in the surface, middle and deep ocean, (c) DIC in the surface middle and deep ocean, (d) carbonate ion concentration of the surface and deep ocean, (e) atmospheric pCO_2, (f) surface and deep ocean alkalinity, (g) surface and deep ocean pH, (h) effective lysocline depth and (i) input (grey line) versus burial fluxes (black line). Surface ocean parameters are indicated with a light grey line, middle ocean parameters with a dark grey line, and deep ocean parameters with a black line. Note that productivity (a) and nutrient concentrations (b) are unaffected during scenarios 1, 2, 5 and 6, whereas they are allowed to covary with F_{riv} by 50% for scenario 4 (stippled line). Modelling results for scenarios 5b and 6b are also indicated by a strippled line. Scenarios 3–6 are associated with carbon input and burial changes (i), causing changes in (c) total dissolved inorganic carbon, (d) carbonate ion, (e) atmospheric pCO_2, (f) alkalinity, (g) pH, and (h) effective lysocline depth (integrated depth of the aragonite–calcite lysocline).

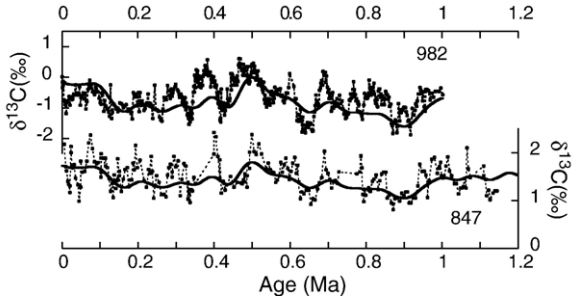

Fig. 6. Long-term planktonic foraminiferal $\delta^{13}C$ records from the Atlantic Ocean (Site 982 [35]) and the Pacific Ocean (Site 847 [36]). The overall trends of the planktonic foraminiferal $\delta^{13}C$ records from these two end-members (North Atlantic versus Pacific) strongly resemble that of $\delta^{13}C_{stacked}$ (thick black line; not to scale).

$\delta^{13}C_{stacked}$ as calculated by the mechanistic box-model after Chuck et al. [23] are summarized in Table 1 for the six scenarios outlined above. Prior to 1.00 Ma, $\delta^{13}C_{stacked}$ variations are presumed to be negligible (Fig. 3), the system is assumed to have been at steady state, and the values used for the various parameters are: $\delta_{riv}=-3.9‰$, $\delta_{org}=-21.5‰$, $F_{riv}=2.40\times10^{14}$ g C yr^{-1}, $F_{org}=4.8\times10^{13}$ g C yr^{-1} and $F_{ino}=1.92\times10^{14}$ g C yr^{-1} after [25].

Our main results for all six scenarios are presented in Figs. 4 and 5. All six scenarios show similar long-term trends in both benthic and planktonic foraminiferal $\delta^{13}C$ as the observations, with decreasing $\delta^{13}C$ values between 1.00 to 0.90 and 0.50 to 0.25 Ma and increasing values between 0.90 to 0.50 and 0.25 to 0.10 Ma (Fig. 4). The surface (planktonic) $\delta^{13}C$ records generally show similar trends to those identified in paleo-records, but variations are observed between the various scenarios (Figs. 4 and 6). As the planktonic $\delta^{13}C$-records reflect conditions in a thin surface layer with a potentially high seasonal, regional and vertical (different planktonic foraminifera species have different depth habitat) variability their use as direct proxies for quantitative changes in surface water $\delta^{13}C$ is less certain.

4. Which scenario fits best?

In scenario 1, relatively large changes in δ_{riv} are needed if they are to drive the $\delta^{13}C_{stacked}$ fluctuations (Table 1). For example, between 0.90 and 0.50 Ma (node 2 and 3), δ_{riv} would have to increase from −4.65 to −3.60‰. If changes in δ_{riv} were the result of changes in the relative weathering rates of inorganic and organic carbon, one would expect this to be reflected in the osmium isotope composition of seawater, as osmium isotopes are sensitive to the ratio of organic carbon weathering to total weathering [26–28], but over the periods considered here no significant fluctuations are apparent [29]. Using shifts in the dominance of terrestrial C3/C4 plants to explain the observed $\delta^{13}C_{stacked}$ fluctuations is more complicated. In order to decrease δ_{riv} a decrease in the abundance of C4 plants at the expense of C3 would be needed. However, such a vegetation shift would result in more ^{12}C being tied up in the terrestrial vegetation, compensating for the effect of the δ_{riv} decrease by decreasing ocean ^{12}C. An abrupt increase in the percentage of C4 plants has been recorded, associated with the shift towards lower $\delta^{13}C$ values during the MPCF [30]. However, Raymo et al. [12] calculate that unreasonably large shifts in the dominance of C3/C4 plants would be needed to explain the $\delta^{13}C$ fluctuations. Hence, scenario 1 seems unlikely.

The changes that would be needed in δ_{org} to explain the $\delta^{13}C_{stacked}$ fluctuations (scenario 2, [Table 1]) are considerable; between 0.90 and 0.50 Ma, (nodes 2 and 3), δ_{org} would need to decrease by 9‰. Methane-related changes in $\delta^{13}C$ are not considered in this study as such changes observed in the more distant geological past happened very rapidly within a few thousand years [4]. δ_{org} could change through variations in fractionation during organic matter formation, which is influenced by sea surface temperature (SST). The coolings associated with the initiation of the MPCF and LPCF [30–32] would, however, tend to cause variations in δ_{org} in the opposite direction to what is needed to explain the observed fluctuations (cooler SST increases the solubility of CO_2, which results in increased fractionation leading to lower δ_{org}) (Table 1). Scenario 2 is therefore unsubstantiated.

In scenario 3 the $\delta^{13}C_{stacked}$ fluctuations are driven by changes in δ_{ino} through nutrient induced changes in surface water productivity. Nutrient supply to the sea surface can be changed in two ways: (1) through changes in fluvial and/or atmospheric input, and (2) through changes in vertical ocean mixing, with increases in mixing causing increased supply of nutrients to the sea surface. At the present day, upwelling contributes up to 20 times more nutrients to the sea-surface than river and atmospheric input [33]. We simulate productivity driven $\delta^{13}C_{stacked}$ fluctuations by changing the vertical mixing constants in the ocean (scenario 3). The induced change to productivity lessens over time as nutrient concentrations adjust (residence time of phosphorus = ~30 kyr in this model). Reductions in $\delta^{13}C_{stacked}$ at the initiation of the MPCF and LPCF are associated with decreases in vertical mixing and thus productivity, whereas the periods characterized with increasing $\delta^{13}C_{stacked}$ are represented by stronger mixing to cause enhanced productivity (Fig. 5, Table 1). Changes in ocean carbonate chemistry and atmospheric pCO_2 are

relatively small (Fig. 5). Scenario 3, however, diverges from the other scenarios by not reproducing similar $\delta^{13}C$ changes in the surface waters (Fig. 4). Instead a small offset is observed as a result of changing the biological pump [34], contrasting the trends that are actually observed in planktonic $\delta^{13}C$ paleo-records (Fig. 6), suggesting scenario 3 is unlikely.

Scenario 4, with the observed $\delta^{13}C$ fluctuations driven by changes in the input of carbon through rivers (F_{riv}), requires changes of up to 27–38% in the magnitude of this flux (Table 1). Increases in F_{riv} result in small increases in carbon burial fluxes, associated with enhanced productivity (Fig. 5). Changes in river input and burial are, however, not equal, as most nutrients are likely removed by near-shore sedimentation processes [37]. In scenario 4a it is presumed that nutrient inputs do not change with changes in F_{riv}, whereas in scenario 4b nutrient input is allowed to covary with F_{riv} by 50%. Both scenarios 4a and 4b are very similar (Fig. 5). Increased productivity associated with increased nutrient input causes a small shallowing of the effective lysocline (Fig. 5). However, the calculated changes in F_{riv} cause unfeasibly large changes in global ocean dissolved inorganic carbon (DIC), alkalinity, atmospheric pCO_2, and pH (Fig. 5). After the second carbon isotope fluctuation (0.50 Ma) the carbonate system is moved to a new state, because the model carbonate system possesses two degrees of freedom, but only one stabilising feedback: carbonate compensation (silicate weathering feedback is not incorporated in the model, as this only becomes important on timescales >1.00 Myr [38]), causing unrealistic changes in pCO_2 and ocean carbon chemistry. If silicate weathering was important on these timescales, then the coolings associated with the initiation of the MPCF and LPCF [30–32] would likely act to lower silicate weathering [39]. It is difficult to obtain accurate records of past variations in river discharge, but there is no evidence to suggest that river input was significantly increased during the initiation of the MPCF and LPCF, and on the contrary some evidence suggests that the initial shift to lower $\delta^{13}C$ values during the MPCF was accompanied by a reduction in discharges [40]. Thus scenario 4 seems unrealistic.

In scenarios 5a and 5b $\delta^{13}C_{stacked}$ fluctuations relate to variations in the organic and inorganic carbon burial fluxes (F_{org} and F_{ino}), either caused by (a) changes in burial preservation or (b) changes in the production- and export rain ratio (ratio between organic and inorganic carbon exported from the sea surface), with the applied changes following the approximate global F_{org} and F_{ino} ratio of 1:4 [25] (Table 1). In scenario 5a $\delta^{13}C_{stacked}$ is forced by explicit variations in F_{org} and F_{ino} by adjusting the stoichiometric ratios of organic and inorganic carbon to phosphorus in the global burial flux (Table 1). These variations occur irrespective of carbonate ion concentration (compensation is prevented) and phosphorus cycling is left unaltered. In scenario 5b carbonate compensation is allowed and it is the production ratio that is varied following a ratio of change of 1:4 (Table 1). In the case where the changes in F_{org} and F_{ino} (Table 1) are forced by changes in burial preservation at a 1:4 ratio without carbonate compensation (scenario 5a) large changes in atmospheric pCO_2, pH, alkalinity and extremely large changes (>3 km) in the effective lysocline depth are apparent (Fig. 5). Although the calcite lysocline may vary by up to ~500 m on glacial/interglacial time scales [5,41–44], on the longer time scale considered here lysocline depth variations are more limited, and only vary by about ±150 m from the present ~4 km [33,45]. We use the integrated depth of the aragonite and calcite lysocline to represent the 'effective lysocline depth'. Long-term changes in the 'effective lysocline depth' may be slightly larger compared with the calcite lysocline, as aragonite is more soluble than calcite, and vary by ±250 m from the present ~2.4 km. The enormous variations in the depth of the effective lysocline resulting from the changes in burial inferred from scenario 5a do not agree with observations. In the case where carbonate compensation is allowed to operate (scenario 5b), variations in atmospheric pCO_2, pH and alkalinity are much reduced (Fig. 5). However, variations in the depth of the effective lysocline (up to 500 m) are still substantial and diverge beyond the ±250 m constraint derived for the period of interest. Scenario 5 therefore seems unrealistic.

Scenario 6 is similar to scenario 5, as $\delta^{13}C_{stacked}$ fluctuations are also considered to be caused by changes in the carbon burial fluxes F_{org} and F_{ino}. However, scenario 6 uses a ratio of change of $\Delta F_{org}:\Delta F_{ino}=1:1$ based on the stoichiometry of the equations $CH_2O+O_2 \Leftrightarrow CO_2+H_2O$ and $CaCO_3+CO_2+H_2O \Leftrightarrow Ca^{+}+2HCO_3^{-}$. The variations in F_{org} and F_{ino} (Table 1) are forced by adjusting the stoichiometric ratios of organic and inorganic carbon to phosphorus in the global burial flux without carbonate compensation (scenario 6a) similar to scenario 5a, and by forcing variations in the production ratio (scenario 6b). In both scenarios 6a and 6b, the invoked changes in F_{org} and F_{ino} (Table 1) cause considerably less variation in atmospheric pCO_2, pH, alkalinity and DIC, and variations in the effective lysocline depth fall within a much narrower range (Fig. 5). Hence, scenario 6, with changes in the carbon burial fluxes while using a ratio of $\Delta F_{org}:\Delta F_{ino}=1:1$, appears to be plausible within the context of the validation criteria.

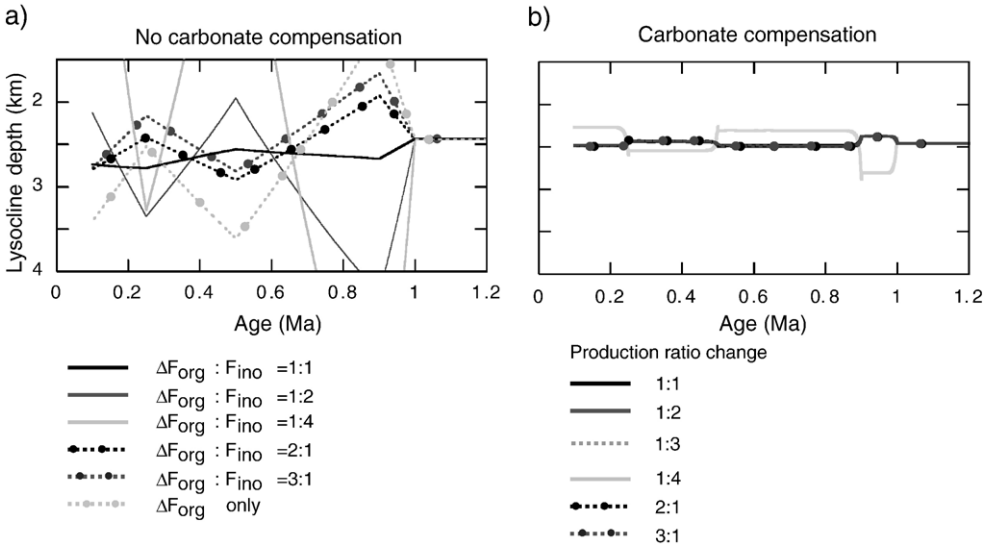

Fig. 7. (a) Comparison of changes in the effective lysocline depth calculated for different burial fluxes with various ΔF_{org}:ΔF_{ino} ratios (1:1, 1:2, 1:4, 2:1, 3:1 and ΔF_{org} changes only). (b) Comparison of changes in the effective lysocline depth calculated for different burial fluxes driven by changes in the production ratio at a 1:4, 1:3, 1:2, 1:1, 2:1 and 3:1 ratio (POC: PIC) of change. Changes that diverge from ΔF_{org}:ΔF_{ino} =1:1 and POC:PIC=1:3 cause unrealistic changes in the depth of the effective lysocline.

From the above discussion, it is predicted that changes in the burial fluxes of organic and inorganic carbon at a 1:1 ratio (scenario 6) are most plausible as the main driver of the long-term $\delta^{13}C_{stacked}$ fluctuations, as ocean carbonate chemistry is not violated, and similar $\delta^{13}C$ changes are reproduced for both deep and surface records (Fig. 4). Changes in the burial fluxes, caused by preservation changes (e.g. scenario 6a) that diverge from this 1:1 ratio invoke larger depth variations in the effective lysocline depth beyond the ±250 m constraint (Fig. 7). Moreover, if changes in the production ratio diverge beyond ΔPOC:ΔPIC=1:3, depth variations in the effective lysocline also become unacceptable (Fig. 7). The modelling results for scenario 6a and 6b imply that long-term changes in atmospheric pCO_2 were small over the past 1.20 Myr (i.e. on time scales exceeding glacial/interglacial cycles).

5. Discussion

The assessment of the various scenarios outlined above indicates that it is most likely that the observed $\delta^{13}C_{stacked}$ fluctuations were driven by carbon burial changes (scenario 6). Although it cannot be excluded that productivity variations also took place simultaneously, these likely were of relatively minor importance, given that large-scale productivity changes would cause an offset between surface and deep $\delta^{13}C$ records, which is not supported by observations (Fig. 6, Supplementary information 1). This evaluation therefore suggests that the changes in the carbon burial fluxes are more likely related to variations in C_{org} and $CaCO_3$ preservation and/or to variations in the production ratio. In the case of changes in the burial fluxes being due to preservation changes (scenario 6a), the question is whether this was mainly related to changes that occur in the water column affecting the export rain rate or upon sediment burial. At the present, the burial efficiency of organic carbon and calcium carbonate is rather low; most organic carbon is remineralized in the upper water column, about 50–75% of the produced calcium carbonate may get dissolved in the upper 1000 m, whereas below 1000 m $CaCO_3$ dissolution is much reduced [46–48]. In upper thermocline waters the ratio of organic carbon to $CaCO_3$ remineralization is about 5 to 1, whereas below ~2 km this ratio decreases to nearly 1:1 [49]. A long-term offset in the surface organic carbon to $CaCO_3$ remineralization ratio could lead to changes in ocean carbon chemistry (e.g. CO_3^{2-} and lysocline depth) and would cause an offset in the vertical $\delta^{13}C$ gradient, which is not observed (Fig. 6). It is therefore most likely that our inferred preservation changes are associated with processes that affect sediments upon burial.

Processes that may affect calcium carbonate contents in sediments are (1) the degree of bottom water saturation with respect to CO_3^{2-}, and (2) respiratory driven dissolution (dissolution of $CaCO_3$ by oxic degradation of organic matter). Long-term changes in bottom water

CO_3^{2-} would influence the position of the lysocline, which is unlikely to have varied by more than ±250 m on these time scales, so this may be an unsuitable mechanism. Respiratory driven dissolution in deep-sea sediments is an important process [50–52], and may be linked to the amount of oxygen available for remineralization of organic material. Increases in the oxygen content of bottom water can greatly increase remineralization of organic carbon and dissolution of $CaCO_3$ [53]. If ca. 1 mol of remineralized organic carbon is used to dissolve 1 mol of $CaCO_3$, the DIC state of bottom waters is not affected to a significant extent.

The model results suggest that, in order to reproduce the $\delta^{13}C$ trends while at the same time avoiding unrealistic lysocline changes, burial fluxes varied in a ratio close to 1:1. This seems unlikely given that at the present time F_{ino} is about 4 times higher than the F_{org} [25]. However, a 1:1 ratio would follow if, on these timescales, $CaCO_3$ dissolution in sediments is controlled by CO_2 supply through release during remineralization of organic carbon. It is unclear from the available evidence whether this is actually the case at a global scale, although the importance of metabolic CO_2 in driving dissolution is recognized [50–52].

There is some evidence to suggest that the oxygen levels of deep-water may have varied over the last 1.20 Myr. During the initiation of the MPCF, Kawagata et al. [54] observe a large decline in the abundance of low oxygen favouring benthic foraminifera from intermediate water depths in the North Atlantic. They suggest this decline may be due to increased dissolved oxygen levels associated with paleoceanographic changes. The main source of dissolved oxygen to the abyss is through the deep conveyor and intensification of deep water formation could form a mechanism to increase dissolved oxygen levels in the deep sea. Alternatively, decreasing deep water temperatures, possibly in response to increasing global ice-volumes, could have resulted in increased deep water oxygen concentrations during the initiation of the MPCF and LPCF.

Our modeling results show that the changes in the burial fluxes can however also be forced through variations in the production- and export ratio. The shifts towards lower $\delta^{13}C_{stacked}$ at the initiation of the MPCF and LPCF would then be associated with slight decreases in the overall production ratio, implying an increase in organic carbon (diatoms) production over calcite (coccoliths and foraminifera). Presently diatom productivity and burial are especially important in the Southern Ocean (south of the Polar Front), the eastern boundary upwelling systems, and the equatorial Pacific. Local increases in diatom productivity may be caused by intensified upwelling and by a northward shift of the Antarctic Polar Front. At the initiation of the MPCF and LPCF, potentially increased upwelling and a northward shift of the polar front in the Southern Ocean [10,55–57] could have promoted local shifts from calcite to silicate production, and may have been responsible for increased opal accumulation rates in the Southern Ocean and along the eastern boundary upwelling systems [58]. Such local production shift would not necessarily cause local offsets in the vertical $\delta^{13}C$ gradient between planktonic and benthic foraminifera, as such a gradient shift depends on the magnitude of change in the POC flux and the localized surface ocean renewal time of ^{12}C through mixing.

The Pleistocene $\delta^{13}C_{stacked}$ is relatively stable prior to the initial excursion of the MPCF at 1.00–0.90 Ma (Fig. 3). A decrease in $\delta^{13}C_{stacked}$ of 0.35‰ between 1.00 and 0.90 Ma (nodes 1 and 2), requires that the total carbon burial flux decreased from 2.40 to 2.22×10^{14} g C yr^{-1} (Fig. 5). During this period there was a larger proportional decrease in organic carbon burial. After 0.90 Ma, $\delta^{13}C_{stacked}$ increased by 0.60‰ until 0.50 Ma. This change requires that the total carbon burial flux increased from 2.22 to 2.44×10^{14} g C yr^{-1} (scenario 6a) or 2.47×10^{14} g C yr^{-1} (scenario 6b) again with a proportional larger increase in organic carbon burial. Similarly, the fluctuation between 0.50 and 0.10 Ma can be achieved by decreasing the total carbon burial flux by 0.8×10^{13} g C yr^{-1} (scenario 6a) or 1.1×10^{13} g C yr^{-1} (scenario 6b) between 0.50 and 0.25 Ma and then increasing it by 1.0×10^{13} g C yr^{-1} (scenario 6a) or 0.9×10^{13} g C yr^{-1} (scenario 6b) between 0.25 and 0.10 Ma (Table 1). If these burial changes resulted from variations in preservation due to respiratory driven dissolution of $CaCO_3$, then the periods of decreasing $\delta^{13}C_{stacked}$ (1.00–0.90 and 0.50–0.25 Ma) would be associated with increased respiratory driven $CaCO_3$ dissolution, whereas the following periods characterized by increasing $\delta^{13}C_{stacked}$ may be linked to periods of reduced respiratory driven dissolution. However, if the burial changes relate to changes in the production ratio, then the periods of lowered $\delta^{13}C_{stacked}$ (1.00–0.90 and 0.50–0.25 Ma) are associated with a decreased production ratio (increase in opal production over calcite), whereas this production ratio would have to increase during periods of increasing $\delta^{13}C_{stacked}$.

The model predicts relative fluctuations in organic and inorganic carbon burial fluxes (F_{org} and F_{ino}) of up to 28% and 6%, respectively. The scale of variations in F_{org} is such that one would expect them to be detectable in areas where there are substantial sedimentary C_{org} concentrations, such as the Sea of Japan, the Barents Sea, parts of the Nordic Sea, the eastern Mediterranean

Sea, the Black Sea, the Arabian Sea, parts of the South Atlantic Ocean, and coastal upwelling areas [59]. Unfortunately, Pleistocene organic carbon burial fluxes are not generally well-documented. We have found only three detailed studies, concerning the eastern Mediterranean, the Sea of Japan and the South Atlantic.

The eastern Mediterranean displays a reduction in the number of preserved organic-rich (sapropel) intervals between 0.98 and 0.58 Ma [60]. As a consequence, we calculate that the amount of organic carbon buried in that basin during the mid-Pleistocene was only about half that buried during intervals with preserved sapropels, while the absence of preserved sapropels between 1.00 and 0.90 Ma defines a total "loss" of $0.6–1.5\times10^{16}$ g C_{org} in the sediments (Supplementary information 3). Although this represents only 1–2% of the total 0.9×10^{18} g decrease in F_{org} projected by our model for that time interval (Table 1), similar C_{org} burial minima also occur in the Sea of Japan [61] and the South Atlantic [62], where preserved C_{org} contents drop from ~4% to ~2% between 0.95 and 0.75 Ma and between 1.10 and 0.85 Ma, respectively. In addition, we note that concomitant calcium carbonate minima occurred around ~1.00 to 0.90 Ma in the South Atlantic, Indian and Pacific Oceans [21,42,55,63].

Thus, the suitable available records all show a broad C_{org} burial flux minimum centred on ~1.00–0.90 Ma, which appears to have coincided with a period of reduced calcium carbonate burial. Those observations are compatible with our hypothesis, which ascribes the initiation of the MPCF (1.00–0.90 Ma) to a global decrease in organic and inorganic carbon burial fluxes, either due to increased respiratory driven dissolution of $CaCO_3$ or a decrease in the production- and export ratio.

Similar support for our hypothesis is found in the case of the LPCF $\delta^{13}C$ shift to low values (0.50–0.25 Ma). It also coincides with a decrease in eastern Mediterranean sapropel preservation [60] and a ~2.5% drop in organic carbon contents in the South Atlantic [62], while a global calcium carbonate low has been described as the Mid-Brunhes dissolution event (~0.40–0.30 Ma) [5,14,21,41,42,56,62,63].

To summarize, it appears that both shifts towards lower $\delta^{13}C_{stacked}$ associated with the initiation of the MPCF and LPCF are characterized by decreases in organic and inorganic carbon burial, supporting our hypothesis that the two long-term $\delta^{13}C$ fluctuations are most likely driven by changes in the organic and inorganic carbon burial fluxes. With the limited amount of information that is available, it is not yet possible to decide what mechanism was mainly responsible for the changes in carbon burial fluxes over the last 1.2 Myr, as there is supporting evidence for both scenarios 6a (preservation changes) and 6b (production ratio changes). It is also possible that the changes in the carbon burial fluxes resulted from a combination of preservation and production ratio changes.

The mid-Pleistocene climate transition (MPT) marked an increase in mean global ice volume and a shift from 41-kyr to 100-kyr ice-age cycles [12]. The exact timing of the MPT, however, remains a matter of debate. Raymo et al. [12] date the MPT between ~920 and 540 ka, Hall et al. [64] report it between 860 and 450 ka, Gingele and Schmieder [65] suggest a start at ~920 ka and termination at ~640 ka, and Henrich et al. [5] propose an early onset at 1200 ka. Clearly, it is important that the timing relationship between the MPT and MPCF is established, since, apart from the glacial cycles themselves, the MPT represents the most fundamental long-term change in Pleistocene climate. Although high frequency glacial/interglacial cycles are associated with relatively large changes in atmospheric pCO_2, the strongest pCO_2 shift inferred by our study for the MPCF (which looks beyond these 'short' term fluctuations) is only ~20 ppmv, which suggests that whatever the timing relationship, the MPT was not driven by a CO_2 shift (Fig. 5). The pCO_2 shift inferred by our study for the LPCF is only ~10 ppmv. The recently published EPICA results confirm relatively stable pCO_2 levels over the last 620 kyr [66]. The present study finds that the MPCF and LPCF were most likely driven by a change in carbon burial, due to preservation changes and/or changes in the production- and export ratio. Both mechanisms are more likely a consequence of a climate transition than a cause. Therefore, it may be expected that the onsets of the MPT and MPCF, as well as the mid-Brunhes event and LPCF, were closely related and coincident.

6. Summary

Carbon isotope records from both surface- and bottom dwelling foraminifera from all major ocean basins show two long-term $\delta^{13}C$ fluctuations between 1.00 and 0.10 Ma. Existing evidence and various hypotheses for these fluctuations are evaluated using the 3-box model of Chuck et al. [23]. Our modeling results suggest that the two long-term $\delta^{13}C$ fluctuations most likely resulted from concomitant changes in the burial fluxes of organic and inorganic carbon. In order to avoid unrealistic changes in the long-term Pleistocene lysocline, the ratio between the amounts of change in organic and inorganic carbon burial would have to be close to a 1:1 ratio. The changes in burial fluxes likely resulted from either deep water ventilation variations causing changes in respiration driven $CaCO_3$ dissolution and/or changes in the production- and export

ratio. Our hypotheses require no fundamental changes in atmospheric pCO_2 associated with the long term $\delta^{13}C$ fluctuations, as corroborated by the recent EPICA pCO_2 reconstruction [66]. It is therefore suggested that the mid-Pleistocene climate transition, which, apart from the glacial cycles, represents the most fundamental change in the Pleistocene climate, was likely not associated with a fundamental change in atmospheric pCO_2.

Acknowledgements

This study used data provided by the Ocean Drilling Program (ODP). ODP is sponsored by the U.S. National Science Foundation (NSF) and participating countries under management of Joint Oceanographic Institutions (JOI), Inc. R. Tiedemann is thanked for making carbon isotope data from Ocean Drilling Program (ODP) Site 659 available. We acknowledge financial support from NERC and the EU program and thank J. Thomson for stimulating discussions. This manuscript was improved through the suggestions of David Archer, Daniel Sigman and several anonymous reviewers, and Peggy Delaney, who served as Editor.

Appendix A. Supplementary Information

Supplementary data associated with this article can be found, in the online version, at doi:10.1016/j.epsl.2006.05.007.

References

[1] L.R. Kump, Interpreting carbon-isotope excursions: strangelove oceans, Geology 19 (1991) 299–302.
[2] E. Vincent, W.H. Berger, Carbon dioxide and polar cooling in the Miocene: the Monterey hypothesis, in: E.T. Sundquist, W.S. Broecker (Eds.), The Carbon Cycle and Atmospheric CO_2: Natural Variation Archean to Present, American Geophysical Union, Washington D.C., 1985, pp. 455–468.
[3] M.L. Delaney, E.A. Boyle, Cd/Ca in late Miocene benthic foraminifera and changes in the global organic carbon budget, Nature 330 (1987) 156–159.
[4] R.D. Norris, U. Röhl, Carbon cycling and chronology of climate warming during the Palaeocene/Eocene transition, Nature 401 (1999) 775–778.
[5] R. Henrich, K.-H. Baumann, R. Huber, H. Meggers, Carbonate preservation records of the past 3 Myr in the Norwegian–Greenland Sea and the northern North Atlantic: implications for the history of NADW production, Marine Geology 184 (2002) 17–39.
[6] R. Tiedemann, M. Sarnthein, N.J. Shackleton, Astronomical timescale for the Pliocene Atlantic $d^{18}O$ and dust flux records of Ocean Drilling Program Site 659, Paleoceanography 9 (1994) 619–638.
[7] D.W. Oppo, M.E. Raymo, G.P. Lohman, A.C. Mix, J.D. Wright, W.L. Prell, A $\delta^{13}C$ record of Upper North Atlantic Deep Water during the past 2.6 million years, Paleoceanography 10 (1995) 373–394.
[8] J. Chen, J.W. Farrell, D.W. Murray, W.L. Prell, Timescale and paleoceanographic implications of a 3.6 m.y. oxygen isotope record from the northeast Indian Ocean (Ocean Drilling Program Site 758), Paleoceanography 10 (1995) 21–48.
[9] A.C. Mix, N.G. Pisias, W. Rugh, J. Wilson, A. Morey, T. Hagelberg, Benthic foraminifera stable isotope record form Site 849, 0–5 Ma: local and global climate changes, in: N.G. Pisias, et al., (Eds.), Proc. ODP, Sci. Res., vol. 138, Ocean Drilling Program, College Station, TX, 1995, pp. 371–412.
[10] P. Wang, J. Tian, X. Cheng, C. Liu, J. Xu, Major Pleistocene stages in a carbon perspective: the South China Sea record and its global comparison, Paleoceanography 19 (2004), doi:10.1029/2003PA000991.
[11] P.M. Kroopnick, The distribution of ^{13}C of $\sum CO_2$ in the world oceans, Deep-Sea Research 32 (1985) 57–84.
[12] M.E. Raymo, D.W. Oppo, W. Curry, The mid-Pleistocene climate transition: a deep-sea carbon isotopic perspective, Paleoceanography 12 (1997) 546–559.
[13] E.A. Boyle, Paired carbon isotope and cadmium data from benthic foraminifera: implications for changes in oceanic phosphorus, ocean circulation, and atmospheric carbon dioxide, Geochimica et Cosmochimica Acta 50 (1986) 265–276.
[14] J.H.F. Jansen, A. Kuijpers, S.R. Troelstra, A mid-Brunhes climatic event: long-term changes in global atmosphere and ocean circulation, Science 232 (1986) 619–622.
[15] P. Wang, J. Tian, X. Cheng, C. Liu, J. Xu, Carbon reservoir changes preceded major ice-sheet expansion at the mid-Brunhes event, Geology 31 (2003) 239–242.
[16] D.W. Lea, J. Bijma, H.J. Spero, D. Archer, Implications of carbonate ion effect on shell carbon and oxygen isotopes for glacial ocean conditions, in: G. Fischer, G. Wefer (Eds.), Use of proxies in Paleoceanography, examples from the South Atlantic, Springer-Verlag, Berlin, 1999, pp. 513–522.
[17] A. Mackensen, L. Licari, Carbon isotopes of live benthic foraminifera from the South Atlantic Ocean: sensitivity to bottom water carbonate saturation state and organic matter rain rates, in: G. Wefer, S. Mulitza, V. Rathmeyer (Eds.), The South Atlantic in the Late Quaternary — Reconstruction of Material Budget and Current Systems, Springer-Verlag, Berlin, 2004, pp. 623–644.
[18] N.J. Shackleton, A. Berger, W.R. Peltier, An alternative astronomical calibration of the lower Pleistocene timescale based on ODP Site 677, Transactions of the Royal Society of Edinburgh: Earth Sciences 81 (1990) 251–261.
[19] L. Tauxe, T. Herbert, N.J. Shackleton, Y.S. Kok, Astronomical calibration of the Matuyama–Brunhes boundary: consequences for magnetic remanence acquisition in marine carbonates and the Asian Loess sequences, Earth and Planetary Science Letters 140 (1996) 133–146.
[20] J. Imbrie, N.J. Shackleton, N.G. Pisias, J.J. Morley, W.L. Prell, D.G. Martinson, J.D. Hays, A. McIntyre, A.C. Mix, The orbital theory of Pleistocene climate: support from a revised chronology of the marine $\delta^{18}O$ record, in: A. Berger, J. Imbrie, J. Hays, G. Kukla, B. Salzmann (Eds.), Milankovich and Climate: understanding response to astronomical forcing 1, D. Reidel Publishing Company, Dordrecht, 1984, pp. 269–305.
[21] F.C. Bassinot, L. Beaufort, E. Vincent, L.D. Labeyrie, F. Rostek, P.J. Müller, X. Quidelleur, Y. Lancelot, Coarse fraction fluctuations in pelagic carbonate sediments from the tropical Indian Ocean: a 1500-kyr record of carbonate dissolution, Paleoceanography 9 (1994) 579–600.

[22] N.J. Shackleton, The carbon isotope record of the Cenozoic: history of organic carbon burial and of oxygen in the ocean and atmosphere, in: J. Brooks, A.J. Fleet (Eds.), Marine Petroleum Source Rocks, Geological Society Special Publication, vol. 26, 1987, pp. 423–434.
[23] A. Chuck, T. Tyrrell, I.J. Totterdell, P.M. Holligan, The oceanic response to carbon emissions over the next century: investigation using three ocean carbon cycle models, Tellus B 57 (2005) 70–86.
[24] D.M. Sigman, D.C. McCorkle, W.R. Martin, The calcite lysocline as a constraint on glacial/interglacial low-latitude production changes, Global Biogeochemical Cycles 12 (1998) 409–427.
[25] M.L. Delaney, E.A. Boyle, Tertiary paleoceanic chemical variability: unintended consequences of simple geochemical models, Paleoceanography 3 (1988) 137–156.
[26] G. Ravizza, B.K. Esser, A possible link between the seawater osmium isotope record and weathering of ancient sedimentary organic matter, Chemical Geology 107 (1993) 255–258.
[27] B. Peucker-Ehrenbrink, R.E. Hannigan, Effects of black shale weathering on the mobility of rhenium and platinum group elements, Geology 28 (2000) 475–478.
[28] B. Peucker-Ehrenbrink, G. Ravizza, The marine osmium isotope record, Terra Nova 12 (2000) 205–219.
[29] G. Ravizza, Variations of the $^{187}Os/^{186}Os$ ratio of seawater over the past 28 million years as inferred from metalliferous carbonates, Earth and Planetary Science Letters 118 (1993) 335–348.
[30] E. Schefuβ, S. Schouten, J.H.F. Jansen, J.S. Sinninghe Damsté, African vegetation controlled by tropical sea surface temperatures in the mid-Pleistocene period, Nature 422 (2003) 418–421.
[31] T. de Garidel-Thoron, Y. Rosenthal, F. Bassinot, L. Beaufort, Stable sea surface temperatures in the western Pacific warm pool over the past 1.75 million years, Nature 433 (2005) 294–298.
[32] E.L. McClymont, A. Rosell-Melé, Links between the onset of modern Walker circulation and the mid-Pleistocene climate transition, Geology 33 (2005) 389–392.
[33] W.S. Broecker, T.H. Peng, Tracers in the Sea, Lamont–Doherty Geological Observations, Columbia University, New York, 1982. 690 pp.
[34] B.K. Sen Gupta, Modern Foraminifera, Kluwer Academic, Dordrecht, 1999. 371 pp.
[35] K.A. Venz, D.A. Hodell, C. Stanton, D.A. Warnke, A 1.0 Myr record of glacial North Atlantic intermediate water variability from ODP site 982 in the northeast Atlantic, Paleoceanography 14 (1999) 42–52.
[36] J.W. Farrell, D.W. Murray, V.S. McKenna, A.C. Ravelo, Upper ocean temperature and nutrient contrast inferred from Pleistocene planktonic foraminifer $\delta^{18}O$ and $\delta^{13}C$ in the eastern equatorial Pacific, in: N.G. Pisias, et al., (Eds.), Proc. ODP Sci., Results, vol. 138, Ocean Drilling Program, College Station, TX, 1995, pp. 289–319.
[37] S.W. Nixon, J.W. Ammerman, L.P. Atkinson, V.M. Berounsky, G. Billen, W.C. Boicourt, W.R. Boynton, T.M. Church, D.M. Ditoro, R. Elmgren, J.H. Garber, A.E. Giblin, R.A. Jahnke, N.J.P. Owens, M.E.Q. Pilson, S.P. Seitzinger, The fate of nitrogen and phosphorus at the land-sea margin of the North Atlantic Ocean, Biogeochemistry 35 (1996) 141–180.
[38] W.S., Broecker, T.H., Peng, 1998. Greenhouse puzzles, Part I, Keeling's World: Is CO_2 Greening the Earth? Eldigio Press, Lamont–Doherty Earth Observatory of Columbia University, Palisades, New York, 111 pp.
[39] M. Meybeck, Pathways of major elements from land to ocean through rivers, in: J.M. Martin, J.D. Burton, D. Eisma (Eds.), Proceedings of the review and workshop on river inputs to ocean-systems, FAO, Rome, 1980, pp. 18–30.
[40] L.M. Dupont, B. Donner, R. Schneider, G. Wefer, Mid-Pleistocene environmental change in tropical Africa began as early as 1.05 Ma, Geology 29 (2001) 195–198.
[41] L.C. Peterson, W.L. Prell, Carbonate preservation and CO_2: natural variations Archean to Present, in: E.T. Sundquist, W.S. Broecker (Eds.), The Carbon Cycle and Atmospheric CO_2: Natural Variation Archean to Present, Am. Geophys. Un., Washington D.C., 1985, pp. 251–269.
[42] J.W. Farrell, W.L. Prell, Pacific $CaCO_3$ preservation and $\delta^{18}O$ since 4 Ma: paleoceanic and paleoclimatic implications, Paleoceanography 6 (1991) 485–498.
[43] N.R. Catubig, D.E. Archer, R. Francois, P. deMenocal, W. Howard, E.-F. Yu, Global deep-sea burial of calcium carbonate during the last glacial maximum, Paleoceanography 13 (1998) 298–310.
[44] A.N.A. Volbers, R. Henrich, Late Quaternary variations in calcium carbonate preservation of deep-sea sediments in the northern Cape Basin: results from a multiproxy approach, Marine Geology 180 (2002) 203–220.
[45] D.K. Rea, M. Leinen, Neogene history of calcite compensation depth and lysocline in the South Pacific Ocean, Nature 316 (1985) 805–807.
[46] J.D. Milliman, P.J. Troy, W.M. Balch, A.K. Adams, Y.-H. Li, F.T. Mackenzie, Biologically mediated dissolution of calcium carbonate above the chemical lysocline? Deep Sea Research I (46) (1999) 1653–1669.
[47] R.A. Feely, C.L. Sabine, K. Lee, F.J. Millero, M.F. Lamb, D. Greeley, J.L. Bullister, R.M. Key, T.H. Peng, A. Kozyr, T. Ono, C.S. Wong, In situ carbonate dissolution in the Pacific Ocean, Global Biogeochemical Cycles 16 (2002), doi:10.1029/2002GB001866.
[48] J.D. Milliman, A.W. Droxler, Neritic and pelagic carbonate sedimentation in the marine environment: ignorance is not bliss, Geologische Rundschau 85 (1996) 496–504.
[49] L.A. Anderson, J.L. Sarmiento, Redfield ratios of remineralization determined by nutrient data analysis, Global Biogeochemical Cycles 8 (1994) 65–80.
[50] W.D. Berelson, D.E. Hammond, J. McManus, T.E. Kilgore, Dissolution kinetics of calcium carbonate in equatorial Pacific sediments, Global Biogeochemical Cycles 8 (1994) 219–235.
[51] B. Hales, S. Emerson, D. Archer, Respiration and dissolution in sediments of the Western North Atlantic: estimates from models of in situ microelectrode measurements of porewater oxygen and pH, Deep Sea Research I (41) (1994) 695–719.
[52] B. Hales, S. Emerson, Calcite dissolution in sediments of the Ontong–Java Plateau: in situ measurements of pore water O_2 and pH, Global Biogeochemical Cycles 10 (1996) 527–541.
[53] D.E. Archer, J.L. Morford, S.R. Emerson, A model of suboxic sedimentary diagenesis suitable for automatic tuning and gridded global domains, Global Biogeochemical Cycles 16 (2002), doi:10.1029/2000GB001288.
[54] S. Kawagata, B.W. Hayward, H.R. Grenfell, A. Sabaa, Mid-Pleistocene extinction of deep-sea foraminifera in the North Atlantic Gateway (ODP sites 980 and 982), Palaeogeography, Palaeoclimatology, Palaeoecology 221 (2005) 267–291.
[55] F. Schmieder, T. von Dobeneck, U. Bleil, The Mid-Pleistocene climate transition as documented in the deep South Atlantic Ocean: initial, interim state and terminal event, Earth Planet Science Letters 179 (2000) 539–549.

[56] T.J. Crowley, Quaternary carbonate changes in the north Atlantic and Atlantic/Pacific comparisons, in: E.T. Sundquist, W.S. Broecker (Eds.), The Carbon Cycle and Atmospheric CO_2: Natural Variation Archean to Present, Am. Geophys. Un, Washington D. C, 1985, pp. 271–284.

[57] S. Becquey, R. Gersonde, Past hydrographic and climatic changes in the Subantarctic Zone of the South Atlantic — the Pleistocene record for ODP Site 1090, Palaeogeography, Palaeoclimatology, Palaeoecology 182 (2002) 221–239.

[58] G. Cortese, R. Gersonde, C.D. Hillenbrand, G. Kuhn, Opal sedimentation shifts in the World Ocean over the last 15 Myr, Earth and Planetary Science Letters 224 (2004) 509–527.

[59] S. Kempe, Carbon in the Rock Cycle, in: B. Bolin, et al., (Eds.), The Global Carbon Cycle SCOPE, vol. 13, John Wiley and Sons, Chichester, 1977, pp. 354–358.

[60] M. Rossignol-Strick, M. Paterne, F.C. Bassinot, K.C. Emeis, H.J. De Lange, An unusual mid-Pleistocene monsoon period over Africa and Asia, Nature 392 (1998) 269–272.

[61] R. Stein, R. Stax, Late Cenozoic changes in flux rates and composition of organic carbon at Site 798, 799 (Sea of Japan), in: K.A. Pisciotto, et al., (Eds.), Proc. ODP Sci. Results 127/128, Part I, Ocean Drilling Program, College Station, TX, 1992, pp. 423–437.

[62] W. Dean, J. Gardner, Cyclic variations in calcium carbonate and organic carbon in Miocene to Holocene sediments, Walvis Ridge, South Atlantic Ocean, in: K.J. Hsü, H.J. Weissert (Eds.), South Atlantic Paleoceanography, 1985, pp. 61–78.

[63] G.A. Haddad, A.W. Droxler, D. Kroon, D.W. Müller, Quaternary $CaCO_3$ input and preservation within Antarctic intermediate water: mineralogic and isotopic results from holes 818B and 817A, Townsville trough (north-eastern Australia margin), in: J.A. McKenzie, et al., (Eds.), Proc. ODP Sci., Results, vol. 133, Ocean Drilling Program, College Station, TX, 1993, pp. 203–225.

[64] I.R. Hall, I.N. McCave, N.J. Shackleton, G.P. Weedon, S.E. Harris, Intensified deep Pacific inflow and ventilation in Pleistocene glacial times, Nature 412 (2001) 809–812.

[65] F.X. Gingele, F. Schmieder, Anomalous South Atlantic lithologies confirm global scale of unusual mid-Pleistocene climate excursion, Earth Planetary Science Letters 186 (2001) 93–101.

[66] U. Siegenthaler, T.F. Stocker, E. Monnin, D. Lüthi, J. Schwander, B. Stauffer, D. Raynaud, J.-M. Barnola, H. Fischer, V. Masson-Delmotte, J. Jouzel, Stable carbon cycle–climate relationship during the late Pleistocene, Science 310 (2005) 1313–1317.